Piezo-free full-field OCT imaging of static biological samples

Hoang Thong Truong,[1] Egan Bauersfeld,[3] and Jesse Wilson[1,2,*]
[1]*Department of Electrical and Computer Engineering, Colorado State University*
[2]*School of Biomedical Engineering, Colorado State University*
[3]*Integrated Design Engineering, College of Engineering and Applied Science, University of Colorado Boulder*
**jesse.wilson@colostate.edu*

ABSTRACT

Full-field optical coherence tomography is a non-invasive imaging technique that can provide volumetric reconstructions of biological samples. Conventionally, full-field optical coherence tomography employs a precise piezoelectric actuator to cycle the reference phase and enable image reconstruction one z-plane at a time. This study revisits an alternative approach using amplitude demodulation on full z-stacks, acquired through constant velocity scanning of static biological samples. Here, we demonstrate the capability of this method to reconstruct 3D volumetric data of a leaf.

Keywords: full-field optical coherence tomography, signal processing, demodulation, biological imaging, tissues

1. INTRODUCTION

Traditional FFOCT systems commonly employ the phase-stepping algorithm, typically a four-phase shifting approach, to reconstruct high-resolution images [1]. This method involves modulating the reference mirror with a piezoelectric actuator (PZT) to introduce phase shifts of π/4, enabling the acquisition of interferograms at four consecutive phases for a given depth. While proven to be effective and fast, the phase-stepping method requires a precise setup with synchronization between the PZT movement, translation stage, and the camera.

A simple alternative, yet often overlooked, approach involves amplitude demodulation on full z-stacks, previously explored for cultural heritage artifact imaging [2]. Rather than shifting phase at each z-plane with a PZT, the method scans the sample through the coherence plane at constant velocity, resulting in interference fringes with respect to the z-axis that can be demodulated with bandpass filtering and rectification to produce an image. Often, a form of adaptive filtering is used to compensate for vibrations and fluctuations in scan velocity [3,4].

Despite its potential, this amplitude demodulation approach has been underutilized for biological samples. Amplitude demodulation is inapplicable to *in vivo* imaging due to the drift between the subject and instrument, thus the requirement for rapid PZT phase shifting. ~~For static~~ tissue samples, this is not a concern.

In this paper, we analyze and present the results of volumetric imaging of a honey locust leaf, using PZT-free amplitude demodulation, with a feedback-stabilized translation stage. We find this produces acceptable image quality even without the use of adaptive filtering.

2. METHODS

As demonstrated in [3], the FFOCT signal at a fixed lateral point (x, y) is modeled as a low-coherence interferometric signal dependent on the depth coordinate z, is defined as:

$$s(z) = A(z)\cos\Phi(z) + n(z)$$

where $A(z)$ represents the fringe envelope containing useful information of the reflections of each tissue layer, $n(z)$ accounts for random noise, and the fringe phase $\Phi(z)$ can be expressed as:

$$\Phi(z) = 2\pi f_c z + \phi + \delta\phi(z)$$

where f_c is carrier frequency of the object, initial phase ϕ, and random phase variations $\phi(z)$. The objective of our method is to extract the fringe envelope $A(z)$, which reflects the scattering properties of the tissue. The amplitude demodulation process begins with band-pass filtering of the signal $s(z)$ to suppress the background component and high-frequency noise. The filter bandwidth is designed to extract relevant data near the expected carrier frequency, which contains all the useful information of the samples. The filtered signal is then squared to isolate the envelope, yielding:

$$s^2(z) = \frac{1}{2}A^2(z)[1 + \cos 2\Phi(z)] = \frac{1}{2}A^2(z) + \frac{1}{2}A^2(z)\cos 2\,\Phi(z).$$

The first term, $\frac{1}{2}A^2(z)$, contains the desired envelope information, while the second term, oscillating at twice the carrier frequency, varies more rapidly. A low-pass filter is subsequently applied to remove the high-frequency component $\frac{1}{2}A^2(z)\cos 2\,\Phi(z)$. Finally, the square root of the filtered signal is computed to recover the envelope $A(z)$ in its original magnitude scale.

3. SETUP

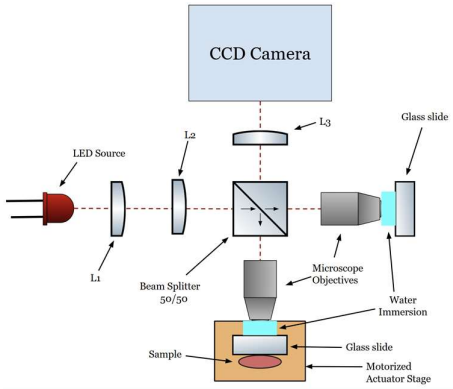

***Figure 1**: FFOCT setup.*

A full-field optical coherence tomography (FFOCT) system is constructed with components mounted on a vibration isolation table. The light source is a 1200 mW LED (Thorlabs M660L4, $\lambda_0 = 660\,nm$, $\Delta\lambda = 20\,nm$). Light is directed through a Kohler illumination ($f_1 = 50$mm, $f_2 = 100$mm) for uniform illumination. The beam splitter splits the light into two beams, guided to the sample and reference arms, each equipped with identical water-immersion objectives (Zeiss W N-Achroplan 10x/0.3 M27, 0.3 NA). A lens ($f_3 = 75.6\,mm$) focuses the sample image onto a CCD camera (Basler aCA1300-30μm). The system achieves an axial resolution 6.97 μm of and a lateral resolution of 1.23 μm. In our setup, we use a glass slide as the reference mirror to ensure similar reflection intensities from the sample and reference arms. On the sample arm, we place the biological sample behind the surface of the glass slide. The sample is placed on a motorized linear actuator (Newport MFA-CC) to perform vertical scanning with a constant velocity.

4. EXPERIMENTS AND RESULTS

We prepared a honey locust leaf for imaging, mounting it on the back of a glass slide with a 774 x 992 µm field of view, the leaf's underside facing the objective. For calibration, we aligned the slide using a HeNe laser to capture interference patterns, then switched to LED sources for OCT imaging. We scanned the sample at a constant velocity using the linear actuator, set to a speed of v =2.475 µm/s. This revealed a carrier frequency of $f_c = 2\,v\,n/\lambda_0$, where n is the refractive index of the sample, and λ_0 is the wavelength of the light source. The resulting carrier frequency was $f_c = 10.5$ Hz,

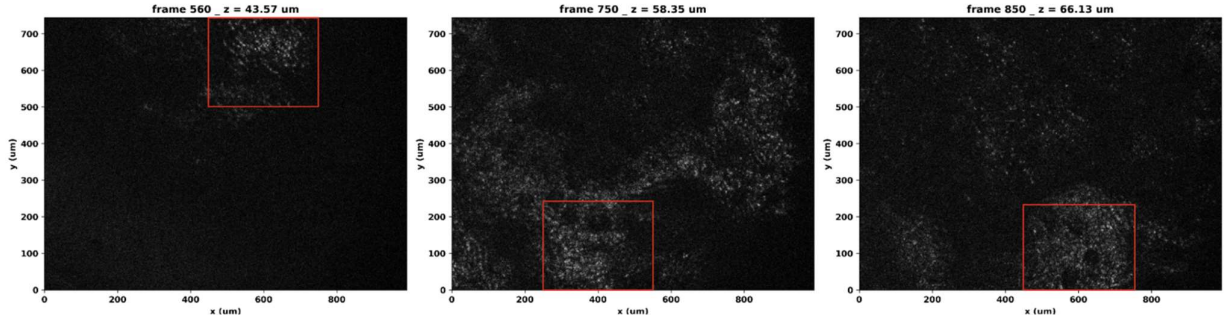

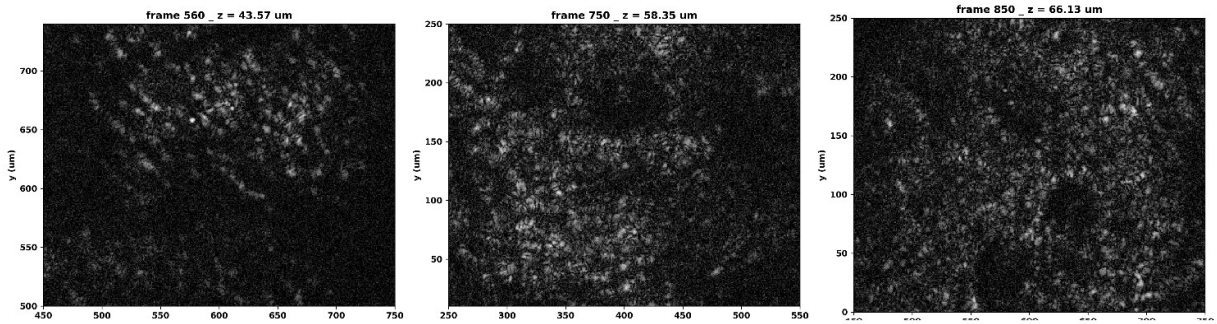

***Figure 2**: Demodulated signals at three different depths, at 43.57 µm,.58.35 µm, and 66.13 µm (top), and their respective zoomed-in images (bottom).*

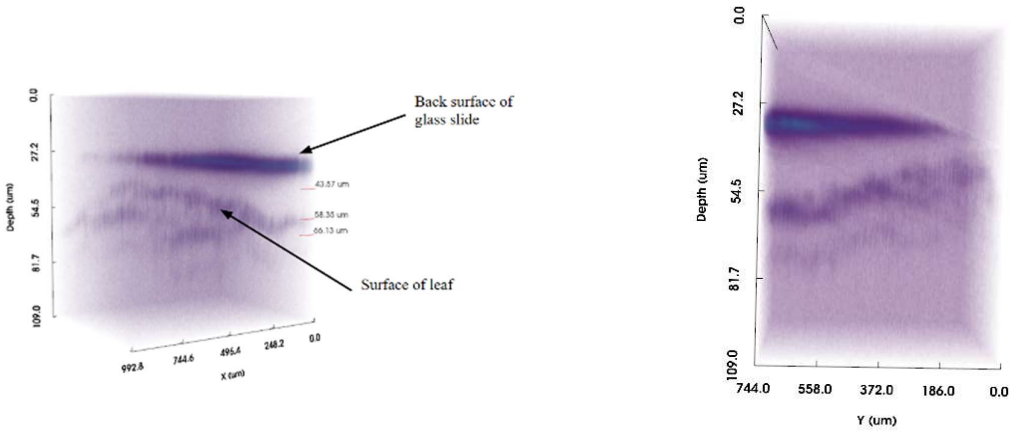

***Figure 3**: The side surfaces of x-z plane (left) and y-z plane (right) of the volumetric data are shown. The darker region corresponds to the back surface of the glass slide, with the volumetric data of the leaf visible below.*

below the Nyquist limit for our camera's maximum frame rate of 31.8 fps. At this velocity, we recorded a video sequence of 2500 frames of raw data, corresponding to a sample depth of 193 µm, with the scanning process completed in 78 seconds.

5. CONCLUSION

This study revisited an underutilized alternative to traditional phase-stepping FFOCT systems: amplitude demodulation via constant velocity scanning, combined with simple bandpass filtering and rectification. Using a feedback-stabilized motor and vibration isolation table, we found acceptable reconstruction quality, even without the computational overhead of adaptive filtering. This proves the potential of this method in laboratory imaging of static biological samples.

REFERENCES

1. Wang, L., Fu, R., Xu, C., & Xu, M. (2022). Methods and applications of full-field optical coherence tomography: a review. *Journal of biomedical optics*, *27*(5), 050901. https://doi.org/10.1117/1.JBO.27.5.050901
2. Volynsky, M., Gladkova, E., Gurov, I., Zhukova, E., Margarian's, N., Sirro, S., & Skakov, P. (2021). Condition diagnosing easel tempera paintings by the high-resolution optical coherence tomography method. Journal of Optical Technology, 88(8), 435–440. https://doi.org/10.1364/JOT.88.000435
3. Gurov, I. (2016). Signal processing methods in full-field optical coherence microscopy. In A. Dubois (Ed.), Handbook of Full-Field Optical Coherence Microscopy: Technology and Applications (pp. 183–222). Pan Stanford Publishing.
4. I. Gurov, V. Kapranova, and P. Skakov, "Dynamical evaluation of interference fringe parameters by the Wiener adaptive filtering method," Appl. Opt. 60, 6799-6808 (2021).